

The early evolution of the star cluster mass function

M. Gieles^{1*}

¹ *European Southern Observatory, Casilla 19001, Santiago 19, Chile*

Accepted 2009 January 6. Received 2009 January 6; in original form 2008 December 4

ABSTRACT

Several recent studies have shown that the star cluster initial mass function (CIMF) can be well approximated by a power law, with indications for a steepening or truncation at high masses. This contribution considers the evolution of such a mass function due to cluster disruption, with emphasis on the part of the mass function that is observable in the first ~ 1 Gyr. A Schechter type function is used for the CIMF, with a power law index of -2 at low masses and an exponential truncation at M_* . Cluster disruption due to the tidal field of the host galaxy and encounters with giant molecular clouds flattens the low-mass end of the mass function, but there is always a part of the ‘evolved Schechter function’ that can be approximated by a power law with index -2 . The mass range for which this holds depends on age, τ , and shifts to higher masses roughly as $\tau^{0.6}$. Mean cluster masses derived from luminosity limited samples increase with age very similarly due to the evolutionary fading of clusters. Empirical mass functions are, therefore, approximately power laws with index -2 , or slightly steeper, at all ages. The results are illustrated by an application to the star cluster population of the interacting galaxy M51, which can be well described by a model with $M_* = (1.9 \pm 0.5) \times 10^5 M_\odot$ and a short (mass-dependent) disruption time destroying M_* clusters in roughly a Gyr.

Key words: galaxies: star clusters – open clusters and associations: general – globular clusters: general

1 INTRODUCTION

The survival chances of young ($\lesssim 1$ Gyr) star clusters and how this may, or may not, depend on their mass, M , and environment has been the topic of quite some debate recently. Two models for the early evolution of clusters have recently become available, with a very different role of M in the disruption description: a mass-dependent disruption model (Boutloukos & Lamers 2003, hereafter BL03; Lamers et al. 2005a; Lamers, Gieles & Portegies Zwart 2005b) and a mass-independent disruption model (Fall et al. 2005; Whitmore et al. 2007). Both disruption models assume a continuous power law cluster initial mass function (CIMF) with index -2 , based on empirical derivations of the mass function of young (~ 10 Myr) clusters with masses between $\sim 10^2 M_\odot$ and $\sim 10^5 M_\odot$ in a variety of galactic environments (see for example Zhang & Fall (1999) for the case of the clusters in the Antennae galaxies; Bik et al. (2003) for clusters in M51; McCrady & Graham (2007) for cluster in M82;

de Grijs & Goodwin (2008) for the SMC and de Grijs et al. (2003a) for a compilation of clusters in different galaxies)¹.

Based on a study of the age and mass distributions of star clusters in four different galaxies, BL03 conclude that the lifetime of star clusters, or disruption time-scale, t_{dis} , depends on M as $t_{\text{dis}} \propto M^\gamma$, with $\gamma \simeq 0.62 \pm 0.06$ and with the proportionality constant dependent on galactic environment. This mass-dependent disruption (MDD) model is supported by our theoretical understanding of the disruption of star clusters, since the same scaling of t_{dis} with M , i.e. the same value of γ , was found from N -body simulations of clusters dissolving under the combined effect of internal relaxation and external tides (Baumgardt & Makino 2003; Gieles & Baumgardt 2008), and also for the disruption of clusters due to external perturbations, or ‘shocks’. In fact, t_{dis} due to shocks depends on both M and the half-mass radius, r_h , since t_{dis} scales with the cluster density within r_h (Spitzer 1958; Ostriker et al. 1972), which combined with the shallow dependence of r_h on M for (young) clusters ($r_h \propto M^{0.1}$, e.g. Larsen 2004), leads to a similar value of γ as for tidal disruption.

¹ The observationally derived CIMF from young ($\lesssim 10$ Myr) clusters will be referred to as the CIMF_{emp}. This is because the number of massive clusters younger than ~ 10 Myr is not necessarily sufficient to reveal the shape of the CIMF at high masses. See Section 2.1.1 for more details.

*E-mail: mgieles@eso.org

MDD flattens the low-mass end of the cluster mass function, dN/dM , at old ages. Fall & Zhang (2001) show that for a constant mass-loss rate ($\gamma = 1$), the mass function of a single-age cluster population evolves towards a flat distribution at the low-mass end, independent of the initial shape of the mass function. Such a mass function is in good agreement with that of the Galactic globular cluster system. However, the globular cluster mass function (GCMF) is usually derived from the luminosity function using a constant mass-to-light ratio, M/L . Mandushev et al. (1991) find from dynamical mass estimates of Galactic globular clusters that their M/L is actually an increasing function of M , which could be the result of the preferential depletion of low-mass stars (Kruijssen & Lamers 2008). Such a mass-dependent M/L alters the shape of the GCMF and could allow for smaller values of γ (Kruijssen & Portegies Zwart, in prep). A general expression for the logarithmic slope at low masses due to MDD is $\gamma - 1$ (Lamers et al. 2005a).

An MDD model for the early evolution of star clusters was introduced by BL03. In the four galaxies studied by BL03, only masses for clusters in M33 and M51 were available. The mass functions of clusters in these galaxies were presented for all ages, so no evidence for a flattening of the mass function for a selected set of old clusters was provided, although these integrated mass functions are slightly flatter at low masses than a power law with index -2 . de Grijs et al. (2003b) report a turnover in the mass function of clusters in region B of M82 and they claim that the population is approximately coeval (~ 1 Gyr). This result was later refuted, since from spectroscopic studies a larger age range with a younger mean was found (Konstantopoulos et al. 2008) and the turnover was attributed to detection incompleteness due to the extent of clusters (Smith et al. 2007; Mayya et al. 2008). de Grijs & Anders (2006) determine the mass function of LMC clusters in different age bins and find that it *steepens* with age, from a power law function with an index of -1.8 at ~ 10 Myr to one with an index of -2.2 at ~ 1 Gyr. Piskunov et al. (2008) also report a steeper mass function at older ages for Milky Way open clusters. This steepening is contrary to what is expected from the evolution of a continuous power law CIMF with mass-dependent disruption. Goudfrooij et al. (2004, 2007) show that the intermediate age (few Gyrs) cluster populations of the merger remnants NGC 1316 and NGC 3610, respectively, provide evidence for a turnover in their mass function, based on a flattening of the cluster luminosity function at low luminosities. But these clusters have already evolved over a significant fraction of a Hubble time, so, it is not at all convincing that the mass function of clusters younger than a Gyr gets shallower than a power law with index -2 .

Zhang & Fall (1999) determined the mass function of cluster in the Antennae aged between 25 and 160 Myr and show that it has essentially the same shape as that for the clusters between 2.5 and 6 Myr, namely a power law with index -2 . Fall et al. (2005) show that the age distribution, $dN/d\tau$, of mass limited subsamples of clusters in the Antennae galaxies declines as τ^{-1} . Such an age distribution can result from a constant formation history combined with a 90% disruption fraction each age dex. Together with the similarity of the mass functions at different ages the authors concluded that the disruption of star clusters in the first Gyr is independent of their mass. Several claims have been made that this mass-independent disruption (MID) model also describes the age distribution of clusters in other galaxies, such as the SMC

(Chandar et al. 2006) and M33 (Sarajedini & Mancone 2007), but these results have later been ascribed to detection incompleteness, since luminosity limited cluster samples, not affected by disruption, also have an age distribution that scales approximately as τ^{-1} (Gieles, Lamers & Portegies Zwart 2007).

The consequence of the 90% MID model is that the number of clusters in logarithmic age bins is constant, which for a continuous power law CIMF results in a constant maximum cluster mass in such bins. Gieles & Bastian (2008) showed that this is indeed the case for the Antennae, but through a comparison to cluster populations in six other galaxies, they also show that the cluster population of the Antennae galaxies is unique in that sense. The MID model fails to reproduce the first few 100 Myr of the (mass limited) $dN/d\tau$ in other galaxies (see the discussion in Gieles et al. 2007 and Gieles & Bastian 2008), so it seems not to be a ‘universal’ scenario for cluster evolution, as claimed by Whitmore et al. (2007).

In summary, the MDD model can not reproduce the correct mass functions at old ages and the MID model can not reproduce the correct age distribution at young ages in galaxies other than the Antennae.

This study searches for the explanation of this problem by abandoning an assumption that both models make, namely a continuous power law CIMF. Alternatively, a truncated Schechter (1976) function (equation 1) is considered for the parent distribution from which cluster masses are drawn and this function is evolved with mass-dependent disruption. In Section 2 arguments for the choice of this truncated distribution function are given and its basic properties are presented. In Section 3 an analytical model for evolved Schechter mass functions is presented and a comparison to the cluster population of M51 is provided in Section 4. A discussion and conclusions are given in Section 5.

2 A SCHECHTER FUNCTION FOR THE CLUSTER INITIAL MASS FUNCTION

2.1 The need for a truncation

Assume that initial cluster masses, M_i , are drawn from a Schechter (1976) parent distribution function of the form

$$\frac{dN}{dM_i} = A M_i^{-2} \exp(-M_i/M_*), \quad (1)$$

where M_* is the mass where the exponential drop occurs and A is a constant that scales with the cluster formation rate (CFR). The constant A can also be taken as a function of time, such that equation (1) describes the cluster formation history and thus represents the probability of a cluster with an initial mass between M_i and $M_i + dM_i$ forming at a time between t and $t + dt$. Since A will be assumed to be constant in most cases throughout this study and since the focus will be on the evolution of the mass function the notation dN/dM_i is preferred, though $dN/(dM_i dt)$ would be more precise.

As mentioned in footnote 1, this distribution function for the cluster initial mass function (CIMF) is not necessarily reflected from the empirically derived CIMF (CIMF_{emp}). This is because usually only clusters younger than ~ 10 Myr are used to determine the CIMF_{emp} . This time interval is short compared to the range of cluster ages in a typical cluster population (few Gyrs). When sampling only a low number of clusters from the distribution function

in equation (1), the most massive cluster actually formed, M_{\max} , can be less massive than M_* , and then the truncation is not recognised from the CIMF_{emp}. The analytical form of equation (1) was proposed for the luminosity function galaxies, where L_* (instead of M_*) is the characteristic galaxy luminosity (Schechter 1976). This functional form follows from a stochastic self-similar model for the origin of galaxies from self-gravitating gas (e.g. Press & Schechter 1974). On stellar scales a power law (self-similar) mass spectrum at low masses with an exponential cut-off at high masses also follows from theoretical models of fragmentation in a collapsing molecular cloud (Silk & Takahashi 1979). For a constant cluster formation efficiency the CIMF reflects the shape of the giant molecular clouds (GMCs) and cores from which the clusters form. Collisions between cores within the GMCs and destruction of the most massive cores by the star formation process also leads to a Schechter type (equilibrium) mass function for clusters (McLaughlin & Pudritz 1996).

The choice for a truncation is also motivated by several indications that the high-mass end of the cluster mass function is steeper when a larger age range, and thus a larger total number of clusters, is considered. The most important arguments are discussed below.

2.1.1 The most massive cluster in logarithmic age bins

Hunter et al. (2003) studied the evolution of the most massive cluster mass, M_{\max} , in equally spaced logarithmic age bins, $M_{\max}(\log \tau)$, in the SMC and the LMC. They show that for a continuous power law mass function $M_{\max}(\log \tau)$ increases with age. This is because for a power law mass function with index $-\alpha$, M_{\max} scales with the number of clusters, N , as $M_{\max} \propto N^{1/(\alpha-1)}$. Assuming a constant CFR, the number of clusters per logarithmic unit of age, $dN/d \log \tau$, scales linearly with τ , since $dN/d \log \tau \propto \tau dN/d\tau$, with $dN/d\tau$ constant. In this case $M_{\max}(\log \tau) \propto \tau^{1/(\alpha-1)}$. For $\alpha = 2$ this results in a linear scaling of $M_{\max}(\log \tau)$ with τ . Kumai, Basu & Fujimoto (1993) find such a relation in the $\log(M)$ vs. $\log(\tau)$ plane of clusters in the SMC, LMC, M31 and M33, which they attribute to time-dependent conditions for cluster formation. Elmegreen & Efremov (1997) were the first to suggest that such an increase is purely a statistical effect that arises from sampling cluster masses from a power law function with index -2 . This power law form was suggested for the mass function of cloud cores as the result of the fractal and turbulent nature of the interstellar gas (Elmegreen & Falgarone 1996). This scale-invariant structure of the gas combined with a near constant star formation efficiency then leads to the same simple power law form for the mass function of clusters (Elmegreen & Efremov 1997). For a constant star formation rate (SFR), the number of clusters is set by the time interval that is considered, which then determines the maximum cluster mass that can (on average) be expected. What this means is that the probability of finding the physical conditions, such as density and pressure, to form a massive cluster is determined by the structure of the gas, which can be described by a simple functional form.

Hunter et al. (2003) find $M_{\max}(\log \tau) \propto \tau^{0.7}$ in the SMC and LMC, from which they conclude that $\alpha \simeq 2.4$. However, from direct fits to the CIMF_{emp} de Grijs & Anders (2006) and de Grijs & Goodwin (2008) find indices of $\alpha = 1.8 \pm 0.1$ and $\alpha = 2.00 \pm 0.15$ for the LMC and the SMC, respectively. The difference between the results of Hunter et al. and de Grijs and

co-workers can be explained when a Schechter distribution function (equation 1) is assumed: Hunter et al. (2003) only use the most massive clusters, i.e. close to M_* where the mass function is steeper, whereas the studies of de Grijs et al. use the full mass range of only the youngest clusters, for which $M_{\max} \lesssim M_*$. From this it can be concluded that in these galaxies it takes more than 10 Myr to sample enough clusters from the CIMF to reach M_* . This scenario is confirmed by the results of de Grijs & Anders (2006) who show that the mass function of LMC clusters in different age bins gets steeper with age, from -1.8 ± 0.1 at ~ 10 Myr to -2.2 ± 0.1 at ~ 1 Gyr. Because these mass functions are constructed in equally spaced logarithmic age bins similar arguments hold as above: in the older age bins longer time intervals are considered, thus sampling higher masses from the CIMF where it is steeper. Lastly, Larsen (2008) recently showed that a Schechter function with $M_* = 2 \times 10^5 M_{\odot}$ provides a good description of the high-mass end of the mass function of LMC clusters when the full age range is considered (but excluding the globular clusters).

Gieles & Bastian (2008) also looked at $M_{\max}(\log \tau)$ for clusters in the SMC and LMC (using the data from Hunter et al.) and added cluster populations from five other galaxies. A linear increase of $M_{\max}(\log \tau)$ with τ holds for the Milky Way open clusters and for the clusters in the SMC, LMC, M33 and M83 up to ages of ~ 100 Myr, which implies that $\alpha = 2$ for the mass range (sampled in that age range) in those galaxies. It also means that there has been no disruption of massive clusters in these galaxies in this age range. In the ‘universal’ MID model of Whitmore et al. (2007), 90% of all clusters gets destroyed each age dex, which predicts a constant number of clusters in logarithmic age bins (if $dN/d\tau \propto \tau^{-1}$, then $dN/d \log \tau = \text{constant}$), and therefore a constant M_{\max} in such bins (Gieles & Bastian 2008). Since this is not the case in most of the galaxies, the linear scaling of $M_{\max}(\log \tau)$ with τ is an important argument against the ‘universal’ MID model of Whitmore et al. (2007).

When the full age range of the cluster population is considered, the increase of $M_{\max}(\log \tau)$ with τ is slower than linear, roughly $M_{\max}(\log \tau) \propto \tau^{0.7}$ (Gieles & Bastian 2008), in agreement with what Hunter et al. had found. For clusters in M51 the increase of $M_{\max}(\log \tau)$ with τ is even slower and for the Antennae galaxies $M_{\max}(\log \tau)$ is essentially independent of τ , suggesting that due to the high SFR of these galaxies $M_{\max} \simeq M_*$ already at short intervals of τ , such that $M_{\max}(\log \tau)$ is approximately constant. However, a high MID fraction and a truncation in the CIMF have more or less the same effect on the evolution of $M_{\max}(\log \tau)$ with τ (Gieles & Bastian 2008). In addition, a non-constant formation history of clusters, one which was lower in the past, can also produce a constant $M_{\max}(\log \tau)$. Additional age and mass distributions are needed to tell these effects apart.

In Section 4 it is shown that the truncated CIMF scenario combined with mass-dependent disruption nicely explains the age distribution and mass function of M51 clusters and the MID model is rejected based on the age distribution of massive clusters. However, a truncation in the mass function does not explain the τ^{-1} age distribution of the Antennae clusters.

2.1.2 Variations in the cluster luminosity function

Indirect evidence for a steepening of the cluster mass function at the high-mass end comes from the luminosity function (LF) of clusters.

The LFs of clusters in different galaxies can be well approximated by a power law, but with an index smaller than the index of the CIMF_{emp} (between -2.5 and -2 , e.g. Dolphin & Kennicutt 2002; Elmegreen et al. 2002; Larsen 2002) with the LF being steeper at higher luminosities (Whitmore et al. 1999; Zepf et al. 1999; Benedict et al. 2002; Larsen 2002; Mengel et al. 2005; Gieles et al. 2006a,b; Hwang & Lee 2008). The LF consists of clusters with different ages. Due to the age dependent light-to-mass ratio of clusters, the LF does not necessarily have the same shape as the mass function. However, if the CIMF is a continuous power law with the same index at all ages, i.e. with the physical maximum much higher than M_{max} , the LF will be a power law with the exact same index. Age dependent extinction or bursts in the formation rate would not cause a difference between the CIMF and the LF. An addition of identical power laws always results in the same power law. So the fact that the LF is slightly steeper than the CIMF_{emp} is already a strong indication that the CIMF is not a continuous power law function.

When an abrupt truncation of the CIMF at some mass M_{up} is assumed, it is possible to roughly estimate the index of the bright-end of the LF. Assume that the CIMF is fully populated, i.e. the mass of the most massive cluster actually formed, M_{max} , is equal to M_{up} . Then assume a constant formation history of clusters, so a constant number of the most massive clusters per unit of time: $dN_{\text{up}}/d\tau = \text{constant}$. The luminosities of these clusters, L_{up} , however, depend strongly on age. The light-to-mass ratio, or the flux of a cluster of constant mass, scales roughly with τ as $\tau^{-\zeta}$, with $0.7 \lesssim \zeta \lesssim 1$ depending on the filter, such that $\partial L_{\text{up}}/\partial \tau \propto \tau^{-\zeta-1} \propto L_{\text{up}}^{1+1/\zeta}$. Then the LF of such clusters is

$$\frac{dN_{\text{up}}}{dL_{\text{up}}} \propto \frac{dN_{\text{up}}}{d\tau} \left| \frac{\partial \tau}{\partial L_{\text{up}}} \right| \quad (2)$$

$$\propto L_{\text{up}}^{-1-1/\zeta}, \quad (3)$$

$$\propto L_{\text{up}}^{-2.5}, \quad (4)$$

where in the last step $\zeta = 0.7$ is used (BL03, Gieles et al. 2007), such that the index of -2.5 holds for the V -band LF. The same arguments hold for the luminosities of the 2^{nd} , 3^{rd} , etc. most massive clusters, such that the bright-end of the LF of the entire population is an addition of power law with index -2.5 , resulting in a power law with index -2.5 .

The faint-end of the LF should still be a power law with index -2 or flatter if MDD is important. This double power law shape for the LF was found by Gieles et al. (2006b) and Whitmore et al. (1999) for the LF of clusters in M51 and the Antennae, respectively. When a Schechter function for the CIMF is considered, the logarithmic slope of the LF shows a smooth decline from -2 to roughly -3 between $M_V \simeq -4$ and $M_V \simeq -12$ (Larsen 2008). MDD affects the faint-end ($M_V \gtrsim -8$) of the LF and makes it slightly shallower (index > -2).

2.1.3 The value of M_*

Is the value of M_* universal? Or does it somehow depend on galactic conditions, such as the SFR? The two proxies for the shape of the high-mass end of the CIMF, namely the evolution of $M_{\text{max}}(\log \tau)$ with τ (Section 2.1.1) and the power law index of the LF (Section 2.1.2), both show more convincing signatures of a truncation in the mass function in galaxies with a high SFR.

This suggests that in such environments there are numerous clusters with masses above M_* , as opposed to galaxies with a low SFR. This excludes a linear dependence of M_* on the SFR. If M_* would scale linearly with the SFR, then it would take the same amount of time in each galaxy for M_{max} to reach M_* , since in the power law regime of the Schechter function $M_{\text{max}}(\log \tau) \propto \tau$ (Section 2.1.1). This was suggested by Weidner, Kroupa & Larsen (2004) and Maschberger & Kroupa (2007), who claim a formation epoch of 10 Myr for an entire CIMF. If the CIMF is populated up to the highest mass each 10 Myr, then there should be no increase of $M_{\text{max}}(\log \tau)$ with age (assuming all age bins have a width larger than 10 Myr). But this is not what Hunter et al. (2003) and Gieles & Bastian (2008) find. Weidner et al. (2004) base their result on the relation between the luminosity of the brightest cluster in a galaxy, $M_V^{\text{brightest}}$, with the SFR of that galaxy using data from Larsen (2002) and the assumption that the brightest cluster is also the most massive cluster. They then use a constant light-to-mass ratio to convert luminosities to masses. This assumption was further investigated by Larsen (2008), who determined the ages of all $M_V^{\text{brightest}}$ clusters from Larsen (2002) and showed that the brightest clusters ($M_V^{\text{brightest}} \lesssim -11$) are young ($\lesssim 30$ Myr) while the clusters with $M_V^{\text{brightest}} \gtrsim -11$ have a large age spread (between ~ 10 Myr and ~ 1 Gyr). If the age of $M_V^{\text{brightest}}$ is M_V dependent, then so is the light-to-mass ratio. Assuming that it is constant can thus lead to a misinterpretation of the data. Larsen (2008) showed that the $M_V^{\text{brightest}}$ vs. SFR relation for (quiescent) spiral galaxies is consistent with a constant M_* of $M_* \simeq 2 \times 10^5 M_{\odot}$.

This value of M_* is probably not universal, since there are extremely massive clusters known ($10^7 - 10^8 M_{\odot}$, Maraston et al. 2004; Bastian et al. 2006), which are unlikely to have formed from a Schechter function with $M_* = 2 \times 10^5 M_{\odot}$. Jordán et al. (2007, hereafter J07) determine M_* values of globular cluster populations of early-type galaxies in the Virgo Cluster by comparing the cluster luminosity functions to ‘evolved Schechter functions’. They find a trend of M_* with host galaxy luminosity, with M_* being higher in brighter galaxies, and values for M_* between a few times $10^5 M_{\odot}$ and a few times $10^6 M_{\odot}$. Several other studies have also shown that a Schechter function fits the high-mass end of the globular cluster mass function better than a continuous power law with index -2 (McLaughlin & Pudritz 1996; Burkert & Smith 2000; Fall & Zhang 2001; Waters et al. 2006; Harris et al. 2008).

Billett et al. (2002) suggest there should exist a maximum cluster mass based on the Kennicutt (1998) relation between the SFR and gas density and the assumption of a pressure equilibrium between the ambient interstellar medium and the cloud-cores from which star clusters form. For a constant cluster density this relation is $M_{\text{up}} \propto \text{SFR}^2$ and for a constant cluster radius, it would be $M_{\text{up}} \propto \text{SFR}^{2/3}$. With the latter increase of M_{up} with the SFR, i.e. slower than linear, it is possible to explain the observational trends discussed in Sections 2.1.1–2.1.2. The key point is that M_* is probably environment dependent and for the masses of a cluster population in a given galaxy to be affected by the truncation, the product of the SFR times the age range has to be high. For $M_* \propto \text{SFR}^{2/3}$, low SFR galaxies need longer time intervals for M_{max} to reach M_* than high SFR galaxies, which seems to be what is found from observations. The relation between M_{max} and the SFR will be quantified in more detail in Section 2.2.

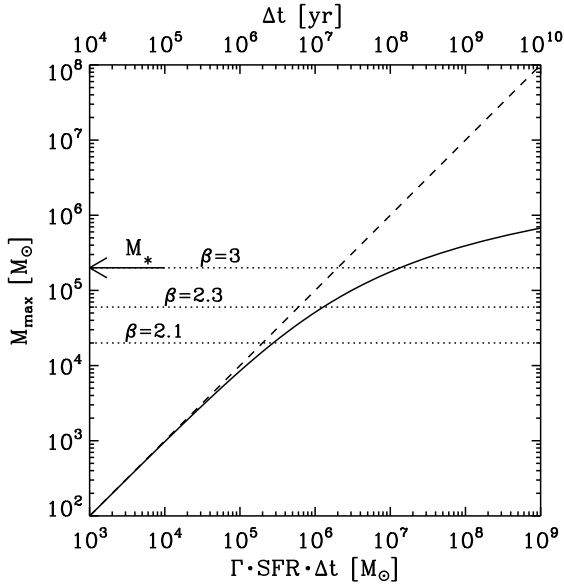


Figure 1. Example of the relation between the mass of the most massive cluster, M_{\max} , as a function of the total mass formed in clusters, $\Gamma \cdot \text{SFR} \cdot \Delta t$, when the CIMF is a Schechter function (equation 1) with $M_* = 2 \times 10^5 M_\odot$ (Larsen 2008). The dashed line shows a prediction for M_{\max} in the case of a nontruncated mass function. The dotted lines indicate three masses and the corresponding logarithmic slope, $-\beta$, of the Schechter function. The top x -axis shows the time range that is needed to form the amount of mass that is represented on the bottom x -axis when $\text{SFR} = 1 M_\odot \text{yr}^{-1}$ and $\Gamma = 0.1$.

2.2 The relation between M_{\max} and the star formation rate

The mass of the most massive cluster in a cluster population, M_{\max} , depends on how many cluster are formed. This can be related to the CFR which scales linearly with the constant A in equation (1), since

$$\text{CFR} = \int_{M_{\min}}^{\infty} M_i \frac{dN}{dM_i} dM_i, \quad (5)$$

$$= A E_1 \left(\frac{M_{\min}}{M_*} \right), \quad (6)$$

$$\simeq 10 A, \quad (7)$$

where $E_n(x)$ with $n = 1$ is a generalised expression of the exponential integral². In the last step $M_{\min}/M_* \simeq 10^{-5}$ is used. For a ratio of $M_{\min}/M_* = 10^{-4}$ (10^{-3}) a relation of $\text{CFR} \simeq 8A$ ($6A$) is found, showing that the relation between the CFR and A is relatively insensitive to the ratio M_{\min}/M_* . The variable A can be a function of time, $A(t)$, to include variations in the CFR. This does not influence the shape of the mass function, but it will affect the

² The exponential integral is defined as $E_n = \int_1^\infty t^{-n} \exp(-xt) dt$, and is related to the (upper) incomplete Gamma function, $\Gamma(a, x)$, as $E_n(x) = x^{n-1} \Gamma(1-n, x)$. See Section 6.3 in Numerical Recipes (Press et al. 1992) for details on the exponential integral and how to implement this function in a code. The exponential integral is predefined in IDL as the function `expint(n, x)`.

shape of the age distribution, which can be derived once the CIMF is evolved with disruption (Section 3).

The relation between M_{\max} and A can be found from

$$1 = \int_{M_{\max}}^{\infty} \frac{dN}{dM_i} dM_i, \quad (8)$$

$$= \frac{A E_2(M_{\max}/M_*)}{M_{\max}}. \quad (9)$$

For $M_{\max} \ll M_*$ the term $E_2(M_{\max}/M_*) \simeq 1$, and $A \simeq M_{\max}$, which is the result for a continuous power law with index -2 . An expression for M_{\max} as a function of the CFR can be found by substituting A as a function of the CFR from equation (6) in equation (9). Since this is then in units of $M_\odot \text{yr}^{-1}$, a multiplication by some time interval, Δt , is necessary to get an expression for M_{\max} in M_\odot . Assuming that a constant fraction Γ of the SFR ends up in star clusters that survive the embedded phase (Bastian 2008), i.e. $\text{CFR} = \Gamma \cdot \text{SFR}$, then a relation between M_{\max} and the SFR is found

$$\frac{M_{\max}}{E_2(M_{\max}/M_*)} = \frac{\Gamma \cdot \text{SFR} \cdot \Delta t}{E_1(M_{\min}/M_*)}. \quad (10)$$

This relation between M_{\max} and $\Gamma \cdot \text{SFR} \cdot \Delta t$ is illustrated in Fig. 1. Since the exponential integral is not easily inverted the product $\Gamma \cdot \text{SFR} \cdot \Delta t$ is calculated for a series of M_{\max} values. A value of $M_* = 2 \times 10^5 M_\odot$ is used, which was found for spiral galaxies by Larsen (2008), and $E_1(M_{\min}/M_*) = 10$, corresponding to $M_{\min} \simeq 1$. The dotted lines indicate three masses where the logarithmic slope of the mass function, $-\beta$, has the values -2.1 , -2.3 and -3 . The logarithmic slope at M of a mass function dN/dM is defined as

$$-\beta(M) \equiv \frac{d \ln(dN/dM)}{d \ln M}, \quad (11)$$

which for the CIMF gives

$$-\beta(M_i) = -2 - M_i/M_*. \quad (12)$$

Note that β is defined such that it is positive for a declining dN/dM .

From Fig. 1 we see that $M_{\max} \simeq 0.1 \Gamma \cdot \text{SFR} \cdot \Delta t$ for $M_{\max} \lesssim 0.1 M_*$. This corresponds to the mass range of the CIMF where $\beta \simeq 2$. For higher values of $\Gamma \cdot \text{SFR} \cdot \Delta t$ the relation between M_{\max} and $\Gamma \cdot \text{SFR} \cdot \Delta t$ flattens. The dashed line shows the predicted M_{\max} for a nontruncated mass function, or a much higher M_* . Even though the two predictions diverge to a difference up to two dex in M_{\max} , a large increase of $\Gamma \cdot \text{SFR} \cdot \Delta t$ (three dex) is needed to reach this difference. When M_{\max} in the CIMF_{emp} is sampled close to or a bit above M_* , the difference between a continuous power law and a Schechter function will be hard to tell. Mainly because the number of clusters in this high-mass tail is low.

The top x -axis of Fig. 1 is labelled with Δt values corresponding to $\Gamma \cdot \text{SFR} \cdot \Delta t$ values with a fixed SFR and Γ of $\text{SFR} = 1 M_\odot \text{yr}^{-1}$ and $\Gamma = 0.1$. These Δt values can be interpreted as age ranges. In this illustrative example of a galaxy with a moderate SFR, the CIMF_{emp} ($\Delta t \lesssim 10 \text{ Myr}$) will contain clusters with masses up to $\sim 5 \times 10^4 M_\odot$, while clusters with masses up to $\sim 10^6 M_\odot$ have formed when an age range of $\sim 10 \text{ Gyr}$ is considered. However, without the exponential truncation clusters with masses up to $10^8 M_\odot$ are predicted to have formed. The example in Fig. 1 can be applied to the Milky Way. Its most massive young star cluster known to date is West-

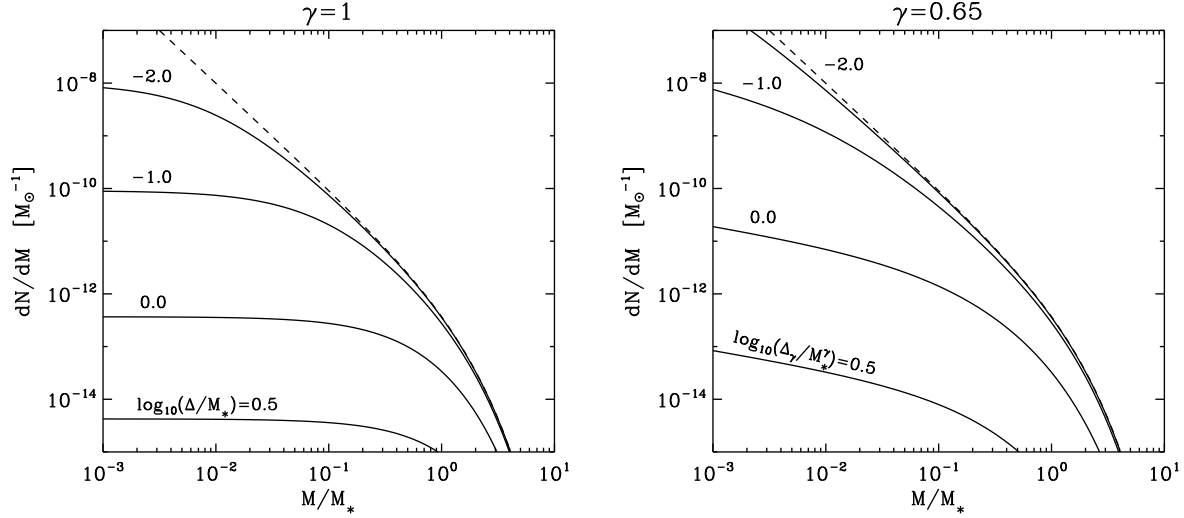


Figure 2. Different stages of the evolved Schechter mass function for a constant mass loss rate (left panel, equation [17]) and a mass-dependent mass loss rate (right panel, equation [26]). The corresponding values of the ratio Δ/M_* (left) and Δ_γ/M_*^γ (right) are indicated. The dashed line in both panels shows the Schechter function at $t = 0$ (equation 1).

erlund 1 which has a mass around $10^5 M_\odot$ (Clark et al. 2005; Mengel & Tacconi-Garman 2007). There are a handful of other massive clusters in the Milky Way known, such as the Arches and Quintuplet cluster towards the Galactic centre, NGC 3603 and the two recently discovered red super giant clusters (Figer et al. 2006; Davies et al. 2007). They are all around $\sim 10^4 M_\odot$ and span an age range of ~ 10 Myr. From Fig. 1 it can be seen that for this age range values of $1 - 5 \times 10^4 M_\odot$ are expected for M_{\max} . If the last Gyr of cluster formation is considered, the Galaxy has probably formed several clusters more massive than Westerlund 1, but not as many, nor as massive compared to the scenario in which the CIMF is a continuous power law.

With the properties of the CIMF introduced, an analytical expression for the ‘evolved Schechter function’, i.e. the cluster mass function after mass-dependent disruption is applied, can now be derived.

3 THE EVOLVED SCHECHTER FUNCTION

In this section the ‘evolved Schechter function’ is presented, based on the CIMF of equation (1) which is evolved with mass-dependent cluster disruption due to e.g. the tidal field of the host galaxy and/or encounters with GMCs. Cluster mass loss due to stellar evolution is not considered at this stage. Also, the power law part of the mass function is always assumed to have an index of -2 for the moment.

It is a simple mathematical exercise to derive all expressions in this section for a variable index and to include the effect of mass loss by stellar evolution, but for reasons of simplicity this is not done in the derivations of the formulae in the coming two sections. In Section 3.3 these two effects are added to the formalism.

3.1 Constant mass loss rate

The evolved Schechter function is first introduced in the form described by J07. The mass loss rate of clusters, \dot{M} , is assumed to be

constant. The disruption time for a cluster of mass M , i.e. the time needed to reach $M = 0$, is then given by

$$t_{\text{dis}} \equiv \frac{M}{\dot{M}}, \quad (13)$$

$$= t_0 M, \quad (14)$$

where in the second step $t_0 \equiv 1/\dot{M}$ is introduced. This linear scaling of t_{dis} with M follows from the assumption that t_{dis} is a constant times the half-mass relaxation time, t_{rh} , and the assumption of a constant cluster half-mass density and a constant Coulomb logarithm in t_{rh} (e.g. Gnedin & Ostriker 1997; Fall & Zhang 2001). A more general expression for the scaling of t_{dis} with M of equation (14) would be $t_{\text{dis}} = t_0 M^\gamma$ (equation 22), with $\gamma = 1$.

The mass evolution of a cluster with time³ is then

$$\begin{aligned} M &= M_i - \dot{M}t, \\ &= M_i - \Delta, \end{aligned} \quad (15)$$

where the variable $\Delta \equiv t/t_0 (= \dot{M}t)$ is introduced, which is a proxy of time, but has the dimension of mass since it is the amount of mass with which M_i has reduced at time t due to disruption.

Though the assumptions that have to be made to arrive to this constant mass loss are arguable, the result is a mathematically appealing description of the evolution of cluster masses, enabling us to make simple analytical predictions. In Section 3.2 a more realistic \dot{M} , based on results of N -body simulations, is explored.

The mass function as a function of time, dN/dM , follows from the conservation of number

$$\frac{dN}{dM} = \frac{dN}{dM_i} \left| \frac{\partial M_i}{\partial M} \right|. \quad (16)$$

³ To keep the formulae synoptic, the variables M and dN/dM , i.e. without the subscript i , are used for to the mass and the mass function as a function of time, i.e. $M(t)$ and $dN/dM(t)$, respectively. The variables M and M_i are in units of M_\odot and t and t_0 are in units of time (Myr).

Since $\partial M_i / \partial M = 1$ and $M_i = M + \Delta$ (equation 15) it then follows that

$$\frac{dN}{dM} = \frac{A}{[M + \Delta]^2} \exp\left(-\frac{M + \Delta}{M_*}\right). \quad (17)$$

The behaviour of this evolved Schechter function is shown in the left panel of Fig. 2. The dashed line shows the CIMF (equation [1] or equation [17] with $\Delta = 0$) and the full lines show the result of equation (17) at different times (i.e. for various ratios of Δ/M_*). For $M \lesssim 0.1\Delta$ and $\Delta \lesssim M_*$ the dN/dM is flat ($\beta = 0$). This is the direct consequence of the constant \dot{M} (Fall & Zhang 2001). The reader is referred to J07 for an equivalent functional form describing the luminosity functions, i.e. the number of clusters in constant magnitude interval, which is peaked and rises at low luminosities.

From equation (17) an expression for the logarithmic slope (equation 11) can be derived

$$-\beta = -2 + \frac{2\Delta}{M + \Delta} - \frac{M}{M_*}. \quad (18)$$

The three terms on the right-hand side are, respectively, the initial index of the power law part of the Schechter function, a disruption term that makes the mass function shallower and a truncation term that makes the mass function steeper. Solving for M gives the mass at which the mass function has the logarithmic slope $-\beta$

$$M(\beta) = \frac{-\Delta + (\beta - 2)M_* + \sqrt{(\Delta + (\beta - 2)M_*)^2 + 8\Delta M_*}}{2}. \quad (19)$$

From this it can be seen that $M(\beta)$ assumes its simplest form when $\beta = 2$. This is where the truncation term in equation (18) equals the disruption term and this could, therefore, be interpreted as a point in the mass function where there is a balance between a steepening due to the truncation and a flattening by disruption. Using equation (19) with $\beta = 2$ an expression for $M(\beta = 2)$ arises

$$M(\beta = 2) = \frac{-\Delta + \sqrt{\Delta^2 + 8\Delta M_*}}{2}. \quad (20)$$

From equation (20) it can be seen that in the limit of $\Delta \ll M_*$, i.e. at young ages where (massive) clusters are not yet affected by disruption, the scaling of $M(\beta = 2)$ with Δ converges to $M(\beta = 2) = \sqrt{2\Delta M_*}$. Since Δ is a proxy for age, it means that the part of the mass function that can be approximated by a power law with index -2 is found at higher masses at older ages. This can also be seen from the expression for β as a function of M and Δ in equation (18). For the mass function to have a logarithmic slope of $\beta = 2$, the two right-hand terms (i.e. the disruption and truncation term) in equation (18) need to have a sum of 0, so Δ is higher at higher masses.

From equation (19) it can be seen that in the same regime of $\Delta \ll M_*$ the behaviour of $M(\beta \neq 2)$ is different. For $\beta < 2$, $M(\beta)$ also increases with Δ , but linearly, so faster than $M(\beta = 2)$. For $\beta > 2$, $M(\beta)$ is constant. This is because at young ages the steep part of the mass function is not affected by disruption at all.

Equation (19) also allows us to find the mass where the mass function, when presented as the number of clusters per logarithmic unit of mass, $dN/d \log M$, peaks or ‘turns over’. This is where $\beta = 1$ and this M is defined as the turnover mass, M_{TO} . Its dependence on aforementioned variables is (J07)

$$M_{\text{TO}} = \frac{-(M_* + \Delta) + \sqrt{(\Delta + M_*)^2 + 4\Delta M_*}}{2}. \quad (21)$$

For $\Delta \ll M_*$ the turnover mass scales as $M_{\text{TO}} \propto \Delta$, like $M(\beta < 2)$, meaning that the turnover shifts to higher masses as time progresses. Notice that due to the different scaling of $M(\beta = 2)$ and M_{TO} with Δ , they approach each other for $\Delta/M_* \gtrsim 1$. In fact, for $\Delta \gg M_*$ the shape of the mass function remains unchanged (J07) and approaches an equilibrium form with $M_{\text{TO}} = M_*$ and $M(\beta = 2) = 2M_*$. The number of clusters reduces as time progresses, but the shape of the evolved Schechter function remains the same. This means that clusters with initial masses much higher than M_* are replacing clusters with lower masses that have already been disrupted. Since the number of clusters above M_* is very low, in practise it means that the total number of remaining clusters quickly drops to 0 after $\Delta = M_*$.

The behaviour of the relations described above is illustrated in the left panel of Fig. 3. It shows M vs. Δ , with both quantities relative to M_* , such that the x and y scales are in dimensionless units of mass and time, respectively. The results for $\beta = 1/1.7/2/2.3$ (equations [19], [20] & [21]) are shown.

The grey shaded region in Fig. 3 shows that there is a large region in the age vs. mass plane, where the logarithmic slope of the mass function equals -2 ± 0.3 . This region more or less coincides with the strip that observed cluster populations occupy in the age-mass plane, implying that the observable part of the evolved Schechter function can be approximated by a power law with index -2 . This will be verified in Section 4 using empirically derived ages and masses of star clusters in M51. But first the case of a mass-dependent mass loss rate is discussed in Section 3.2.

3.2 Mass-dependent mass loss rate

In the previous section a (simplified) linear scaling between t_{dis} and t_{rh} was adopted. However, there are theoretical arguments for a de-coupling of t_{dis} from t_{rh} for clusters dissolving in a tidal field (Fukushige & Heggie 2000). Baumgardt (2001) predicted that $t_{\text{dis}} \propto t_{\text{rh}}^{3/4}$ for clusters that are initially Roche-lobe filling. This leads to a simple scaling of t_{dis} with M of the form (Lamers et al. 2005b)

$$t_{\text{dis}} = t_0 M^\gamma, \quad (22)$$

with t_0 an environment dependent constant and $\gamma \simeq 0.65$. This result for Roche-lobe filling clusters was indeed found from N -body simulations of clusters dissolving in a tidal field (Vesperini & Heggie 1997; Baumgardt & Makino 2003) and it was also found for Roche-lobe underfilling clusters (Gieles & Baumgardt 2008). The simple disruption law of equation (22) was also used to describe age and mass distributions of clusters, from which a mean value of $\gamma = 0.62 \pm 0.06$ was found (BL03).

The mass loss rate, \dot{M} , can be related to t_{dis} as

$$\begin{aligned} \dot{M} &= \frac{M}{t_{\text{dis}}}, \\ &= \frac{M^{1-\gamma}}{t_0}. \end{aligned} \quad (23)$$

For $\gamma \neq 1$ this results in a mass loss rate that is no longer constant, but instead becomes a function of M . Note that then t_0 is not simply $1/\dot{M}$ anymore and that t_{dis} is no longer the time of total disruption as in Section 3.1. The total disruption time, i.e. the time

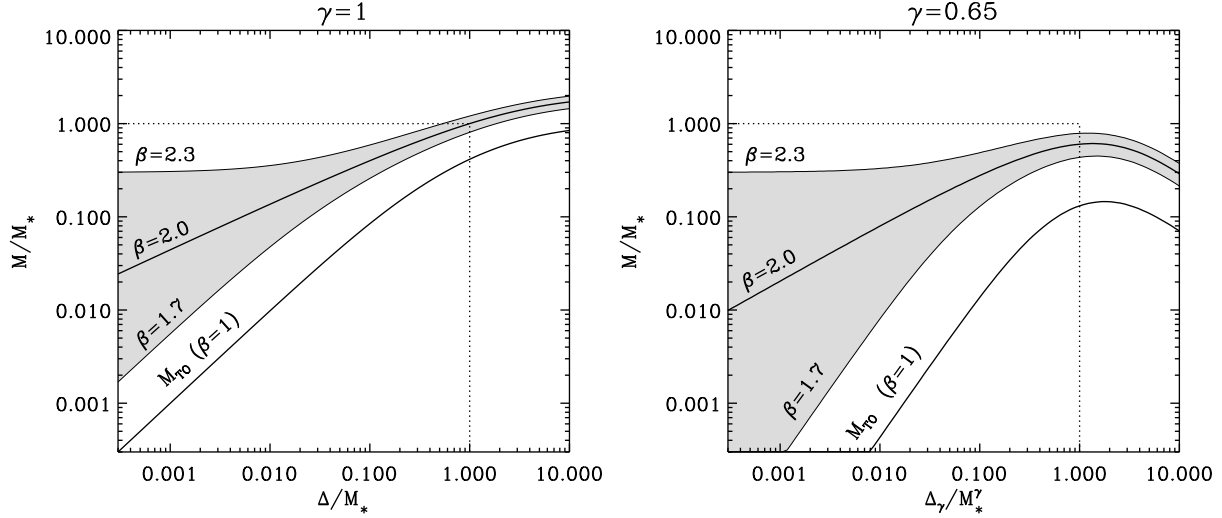


Figure 3. The evolution with age of the mass where the evolved Schechter function has the logarithmic slope, $-\beta$, for different values of β . In the left panel a constant mass loss rate is considered (equation 17, Section 3.1) and in the right panel the mass loss rate depends on mass (equation 26, Section 3.2). The x -axes represent time or age since $\Delta \equiv t/t_0$ and $\Delta_\gamma \equiv \gamma t/t_0$. The mass for which $\beta = 1$, i.e. the mass at which the mass function, presented as the number of clusters in logarithmic mass bins, turns over, is indicated as M_{TO} . The grey shaded region indicates the part of the mass function where the logarithmic slope is -2.0 ± 0.3 .

it takes for all stars to become unbound, will be referred to as $t_{\text{dis}}^{\text{tot}}$. The relation between $t_{\text{dis}}^{\text{tot}}$ and t_{dis} will be derived a bit further down.

With t_{dis} defined as in equation (22) it is still possible to get an analytical expression for the mass evolution with time (Lamers et al. 2005a)

$$M = [M_i^\gamma - \Delta_\gamma]^{1/\gamma}, \quad (24)$$

where Δ_γ is defined as $\Delta_\gamma \equiv \gamma t/t_0$ to get a similar looking expression as in the constant mass loss case (equation 15). The effect of stellar evolution can be taken into account by replacing M_i^γ in equation (24) by $(\mu_{\text{ev}} M_i)^\gamma$, where μ_{ev} is a time-dependent variable that represents the fraction of the initial stellar mass that has not been lost by stellar winds or super-nova explosions (typically between 0.7 and 1). For reasons of simplicity μ_{ev} is not considered in the derivations that follow in this section. In Section 3.3 the results including μ_{ev} are given. The symbol Δ_γ is used when referring to $\gamma < 1$ and Δ is used for the case of $\gamma = 1$. The variable Δ_γ is a proxy of time, like Δ , but note that Δ_γ does not represent the amount of mass that is lost from M_i , like Δ , because of the powers of γ and $1/\gamma$ in equation (24). The instantaneous disruption time for a cluster with mass M is when $\Delta_\gamma/M^\gamma = 1$ (equation 24), such that $t_{\text{dis}}^{\text{tot}}(M) = (t_0/\gamma) M^\gamma$, or $t_{\text{dis}} = \gamma t_{\text{dis}}^{\text{tot}}$.

The partial derivative that is needed (equation 16) to get an expression for the evolved Schechter function can be found from equation (24)

$$\frac{\partial M_i}{\partial M} = \left[1 + \frac{\Delta_\gamma}{M^\gamma} \right]^{1/\gamma-1}, \quad (25)$$

which combined with equation (1) & (16) gives an expression for the evolved Schechter function for a variable γ

$$\frac{dN}{dM} = \frac{A M^{\gamma-1}}{[M^\gamma + \Delta_\gamma]^{(\gamma+1)/\gamma}} \exp\left(-\frac{[M^\gamma + \Delta_\gamma]^{1/\gamma}}{M_*}\right). \quad (26)$$

For $M \ll M_*$ the exponential term in equation (26) is about 1 and the result for a nontruncated mass function of Lamers et al. (2005a) is found, which at low masses and old ages ($M^\gamma \ll \Delta_\gamma$) goes to $dN/dM \propto M^{\gamma-1}$. This is the consequence of the assumed relation between \dot{M} and t_{dis} (equation 23). If \dot{M} was assumed to be constant in time, even when $t_{\text{dis}}^{\text{tot}}(M_i) \propto M_i^\gamma$, with $\gamma < 1$, the low-mass end of the mass function would be flat (index of 0). The shape of the low-mass end of the evolved mass function is thus independent of the shape of the CIMF at those masses and depends only on the way clusters lose mass (Fall & Zhang 2001; Lamers et al. 2005a).

Using the definition of the logarithmic slope, $-\beta$, from equation (11) an expression for β is found

$$-\beta = -2 + \frac{(\gamma+1)\Delta_\gamma}{M^\gamma + \Delta_\gamma} - \frac{M^\gamma (M^\gamma + \Delta_\gamma)^{1/\gamma-1}}{M_*}. \quad (27)$$

Unfortunately equation (27) can only be solved for M analytically for a few specific values of γ and β and the solutions are rather complicated. Therefore, $M(\beta)$ is solved numerically and the right panel of Fig. 3 shows the result for the same values of β as in the constant mass loss case (left panel of Fig. 3) using $\gamma = 0.65$. For $M \ll M_*$, M_{TO} scales as $\Delta_\gamma^{1/\gamma}$, which was also found under the assumption of a continuous power law in the instantaneous disruption model of BL03. However, the increase of M_{TO} with age slows down at high ages, due to the truncation. In contrast to the constant mass loss case, the evolved Schechter function with $\gamma < 1$ does not approach an equilibrium shape. For $\gamma = 0.65$, the value of M_{TO} reaches its highest value ($M_{\text{TO}} \simeq 0.2 M_*$) around $\Delta_\gamma \simeq 2M_*^\gamma$ and then decreases again for older ages. This subtle difference might be important. If globular clusters formed from a Schechter type CIMF, with $M_* \simeq 10^6 M_\odot$, then together with the fact that $M_{\text{TO}} \simeq 2 \times 10^5 M_\odot$, the constant mass loss model would say that the value of M_{TO} can still increase by roughly a factor of five (see left panel of Fig. 3). However, the $\gamma = 0.65$ model shows that M_{TO}

already has its highest possible value when $M_{\text{TO}}/M_* \simeq 0.2$ (right panel of Fig. 3). A possible explanation for the near universality of the value of M_{TO} could thus be that most globular cluster systems have reached already their maximum value of M_{TO}/M_* due to disruption and for a range of roughly an order of magnitude in Δ_γ , the value of M_{TO} will be (within a factor of two) about $0.2 M_*$. Since globular clusters are roughly coeval, a spread in Δ_γ can be interpreted as a spread in disruption time-scales, thereby allowing for a range of t_{dis} values (i.e. different galactocentric distances) resulting in similar values of M_{TO} . Perhaps this adds a piece to the puzzle of the problem of the universality of the globular cluster mass function (see also Ostriker & Gnedin 1997; Vesperini 2000; Whitmore et al. 2002; Baumgardt et al. 2008).

The mass for which the mass function has an index of -2 scales approximately as Δ_γ^η , with $\eta \simeq 0.6$, i.e. slightly different than the $\sqrt{\Delta}$ scaling found for the $\gamma = 1$ case described in Section 3.1⁴. However, the $\Delta_\gamma^{0.6}$ scaling is a bit closer to the increase with age of the limiting mass due to the detection limit, $M_{\text{lim}}(\tau)$, of empirically derived cluster masses. For a V -band detection limit, $M_{\text{lim}}(\tau)$ scales as $\tau^{0.7}$. This implies that the observable part of the evolved Schechter function, i.e. above the detection limit, has a logarithmic slope of approximately -2 at all ages. This is an important result, because it means that there is no significant difference to be expected between the CIMF_{emp} and the shape of the cluster mass function at old ages. So the argument that disruption needs to be mass-independent because old clusters have a similar mass function as young clusters does not hold when a Schechter function is assumed for the CIMF.

All results presented for the constant mass loss case in Section 3.1 are simply a subset of the more general solutions presented in this section. That is, when using $\gamma = 1$, $\Delta_\gamma = \Delta$ and equations (22), (24), (26) & (27) from this section are the same as equations (14), (15), (17) & (18), respectively, from Section 3.1. For completeness a general expression for the evolved Schechter function, including mass loss by stellar evolution and a variable initial power law index, is presented in Section 3.3.

3.3 Including stellar evolution and a variable power law index

As mentioned in the beginning of this section all derivations are done for a fixed power law index of -2 (equation 1) and without the inclusion of mass loss due to stellar evolution. The expressions for the evolved Schechter function and the logarithmic slope $-\beta$ are here given for a variable initial power law index, $-\alpha$, and an additional term μ_{ev} , which is the fraction of the original mass that is not lost due to stellar evolution. Therefore, μ_{ev} is a function of time and can be taken from an SSP model. See also Lamers et al. (2005a) for analytical approximations of $\mu_{\text{ev}}(t)$. Following the same steps as in Section 3.2 the expressions for dN/dM and β are

$$\frac{dN}{dM} = \frac{A \mu_{\text{ev}}^{\alpha-1} M^{\gamma-1}}{[M^\gamma + \Delta_\gamma]^{(\gamma+\alpha-1)/\gamma}} \exp\left(-\frac{[M^\gamma + \Delta_\gamma]^{1/\gamma}}{\mu_{\text{ev}} M_*}\right), \quad (28)$$

and

$$-\beta = -\alpha + \frac{(\gamma + \alpha - 1)\Delta_\gamma}{M^\gamma + \Delta_\gamma} - \frac{M^\gamma (M^\gamma + \Delta_\gamma)^{1/\gamma-1}}{\mu_{\text{ev}} M_*}. \quad (29)$$

From equations (28) & (29) it can be seen that μ_{ev} does not affect the shape of the mass function at low masses, it only affects that vertical offset by a bit. The exponential truncation occurs at slightly lower masses, at $\mu_{\text{ev}} M_*$ instead of M_* .

4 APPLICATION TO M51

To illustrate the cluster population model of the previous section, some of its elements are compared to the cluster population of the interacting galaxy M51 (NGC 5194). The cluster ages and masses were determined from HST/WFPC2 multi-band photometry by Bastian et al. (2005, hereafter B05). The masses are corrected for mass loss by stellar evolution, i.e. they represent the sum of the initial masses of the stars that are still bound in the clusters. The present day masses of the oldest clusters are, therefore, $\sim 25\%$ lower. The M51 cluster population is a good benchmark to test the evolved Schechter function for several reasons: firstly, it is a rich cluster population hosting several massive star clusters (Larsen 2000; B05; Lee et al. 2005; Hwang & Lee 2008). M51 hosts sufficient clusters above $\sim 10^4 M_\odot$, which is the approximate minimum mass for the optical fluxes not to be affected by stochastic effects due to sampling of the stellar IMF, allowing reliable age dating through multi-band photometry (e.g. Cerviño & Luridiana 2004). Secondly, for this cluster population it has been suggested that the mass function is truncated (Gieles et al. 2006b; Haas et al. 2008). Lastly, the disruption time of clusters in M51 is thought to be very short (BL03, Gieles et al. 2005), due to the strong tidal field and the high density of GMCs in the inner region of the galaxy, where most of the clusters of the B05 sample reside. These environmental properties suggest a noticeable evolution of the mass function. Before a comparison between the model and the data is given, the parameters for the CIMF (M_*) and the disruption law (equation 22) are determined in Section 4.1.

4.1 A fit of the evolved Schechter function to the M51 cluster population

If a constant cluster formation history is assumed the evolved Schechter function (equation 26) essentially represents the probability of finding a cluster with mass between M and $M + dM$ and age between τ and $\tau + d\tau$. It can thus be used as a two-dimensional distribution function to determine all the parameters of the evolved Schechter function from empirically derived ages and masses using a maximum likelihood estimate. The only thing which needs to be added is the detection limit. For this the result of the incompleteness analysis of B05 is used, who show that their cluster sample is limited by a detection in the F435W (roughly B) band, for which the 90% completeness fraction is a 22.6 mag. The same simple stellar population (SSP) model was used as in B05 to derive the ages and mass, namely the GALEV models for Salpeter stellar IMF between $0.15 M_\odot$ and $50 M_\odot$ (Schulz et al. 2002; Anders & Fritze-v. Alvensleben 2003). The photometric evolution of a single mass cluster in the F435W band from the SSP model, combined with the 90% completeness limit and the distance to M51 (8.4 Mpc, Feldmeier et al. 1997) then gives the limiting cluster mass as a function of age, $M_{\text{lim}}(\tau)$ (BL03; Gieles et al. 2007).

⁴ In fact, by numerically solving equation (27) for $\beta = 2$ and $0 < \gamma \leq 1$ the relation between η and γ is $\eta \simeq 1 - 0.85\gamma + 0.35\gamma^2$.

This limiting mass, together with the cluster ages and masses, is shown in Fig. 4 and in panel (a) of Fig. 5.

Using $M_{\text{lim}}(\tau)$ and equation (26) artificial models for varying γ , t_0 and M_* are built and a (simultaneous) maximisation of the likelihood of these parameters gives

- $M_* = (1.86 \pm 0.52) \times 10^5 M_\odot$;
- $t_0 = 0.19 \pm 0.10$ Myr;
- $\gamma = 0.67 \pm 0.06$.

The (statistical) uncertainties on each variable are determined using a bootstrap method. For this the original data-set is randomly re-sampled 1000 times, allowing for multiple entries of the same age-mass pair and omission of values, such that the total number of age-mass pairs is the same. The likelihood of the three parameters is determined for each of these 1000 samples and the standard deviation of the results for each parameter is used as the uncertainty.

The disruption parameters (t_0 and γ) imply a total dissolution time for a cluster with an initial mass M_* of $t_*^{\text{tot}} = (t_0/\gamma) M_*^\gamma \simeq 950$ Myr, implying that there should not be many clusters that survive longer than a Gyr. Indeed B05 found only a handful of clusters older than 1 Gyr, although this is probably not only caused by disruption, but also by detection incompleteness. A cluster with an initial mass of $10^4 M_\odot$ gets completely destroyed in $t_4^{\text{tot}} \simeq 130$ Myr. This latter value is in perfect agreement with the results of Gieles et al. (2005), who found $100 \lesssim t_4^{\text{tot}} \lesssim 200$, depending on what is assumed for the cluster formation history. This very short lifetime of clusters in M51, as compared to the lifetime of clusters in the solar neighbourhood or the Magellanic Clouds, was attributed to the high molecular cloud density in this galaxy (Gieles et al. 2006c).

The value of $\gamma = 0.67 \pm 0.06$ agrees perfectly with the mean result of BL03 who found $\gamma = 0.62 \pm 0.06$ from fits to the age and mass distributions of clusters in several galaxies. This value also follows from theory and N -body simulations of clusters dissolving in a tidal field, since for these clusters the disruption time-scale can be expressed as $t_{\text{dis}} \propto (N/\log \Lambda)^{0.75}$ (Baumgardt 2001; Baumgardt & Makino 2003; Gieles & Baumgardt 2008). In this equation, $\log \Lambda \simeq \log(0.1N)$ is the Coulomb logarithm and it follows that this expression for t_{dis} can be well approximated by $t_{\text{dis}} \propto N^{0.62}$ when a relevant range of N is considered (Lamers et al. 2005b). The disruption time due to external perturbations scales (on average) in a similar way with mass. It actually scales linearly with the density of clusters, but since the radius of clusters depends only weakly on their mass, t_{dis} due to external perturbations (GMCs, spiral arms, etc.) also scales as M^γ with γ slightly smaller than 1 (Gieles et al. 2006c; Lamers & Gieles 2006). Gieles et al. (2005) also looked at the mass dependence of cluster disruption in M51 and found that the value of γ depends on the mass range considered. When excluding the most massive clusters ($M \gtrsim 10^5 M_\odot$) a value of $\gamma = 0.6$ was found. Here it is shown that, when considering a Schechter function for the CIMF, the full cluster population can be fit with a disruption law in which t_{dis} depends on mass.

The value of M_* is in excellent agreement with the result of Larsen (2008) who found $M_* = (2.0 \pm 0.5) \times 10^5 M_\odot$ for a sample of spiral galaxies. Gieles et al. (2006b) found a slightly lower value of $M_* = 10^5 M_\odot$ through a model comparison to the LF of M51 clusters. Since the LF is usually constructed for apparent luminosities, i.e. not corrected for local extinction, the derived value of M_* from the LF can be underestimating the true value of M_* .

Gieles et al. (2006b) applied a correction of $A_V = 0.25$ mag to all clusters to roughly account for extinction, but B05 showed that the youngest clusters, which are the brightest ones, are slightly more extinguished than this. Extinction of the brightest clusters has a similar effect on the LF as lowering M_* , so this could be why the value for M_* found by Gieles et al. (2006b) is slightly lower than that found here.

4.2 Logarithmic slopes at different ages

Fig. 4 shows the M51 ages and masses in dimensionless units on top of the predictions for the evolution of several values of β . The results of the maximum likelihood estimation from Section 4.1 are used for the calculation of $M(\beta)$ and the normalisation of age and mass.

The increase of the minimum observable cluster mass, $M_{\text{lim}}(\tau)$, is shown as a dot-dashed line marking the lower envelope of the data points. Most of the clusters fall in the grey region, for which the predicted logarithmic slope of the mass function is -2 ± 0.3 , with the $M(\beta = 2)$ line showing a very similar increase with age as the data points. At old ages $M_{\text{lim}}(\tau)$ approaches the $M(\beta = 2)$ line, implying that the mass function at these ages is somewhat steeper than a -2 power law. Although the disruption time of clusters in M51 is very short, M_{TO} does not get closer than roughly one mass dex below $M_{\text{lim}}(\tau)$ and is, therefore, not observable at any age. The dashed line in Fig. 4 shows $M(\beta = 1.7)$ for the case of a continuous power law CIMF (BL03). This line shows that disruption would clearly make the mass function of the oldest half of the data flatter than a -2 power law if the CIMF was a continuous power law with that index, whereas the $M(\beta = 1.7)$ line for the evolved Schechter function bends down at old ages and stays (almost) below the detection limit.

A direct comparison between the evolved Schechter function (Section 3.2) and the M51 cluster mass functions at different ages is given in Section 4.3.

4.3 Mass functions at different ages

The presentation of cluster ages and masses in dimensionless units in the previous section is not very common. Therefore, the age-mass diagram is presented again, but now in physical units (panel [a] of Fig. 5). Three age bins are created, with boundaries 4, 10, 100 Myr and 600 Myr. The upper boundaries are indicated by τ_1 , τ_2 and τ_3 , respectively. Due to the increasing $M_{\text{lim}}(\tau)$ with τ , three corresponding mass limits are defined as $M_j = M_{\text{lim}}(\tau_j)$, with $1 < j < 3$. The values of M_j are roughly $2 \times 10^3 M_\odot$, $10^4 M_\odot$ and $6 \times 10^4 M_\odot$.

The empirical mass functions in different age bins are shown in panels (b)-(d) of Fig. 5. In each panel an arrow denotes the lower mass limit of each sample, M_j . The first mass bin starts at this lower limit and the number of clusters in each mass bin is counted and then divided by the width of the bin, such that dN/dM is obtained. The dN/dM is also divided by the age range of the sample. In this way the histogram points represent the number of clusters per unit of mass and time/age, or $dN/(dM d\tau)$, which can be compared to the evolved Schechter function. The variables for γ , t_0 and M_* as determined in Section 4.1 are used for the model predictions.

The dashed lines show the CIMFs (equation 1) and the evolved Schechter functions (full lines, equation 26) are based on the mean

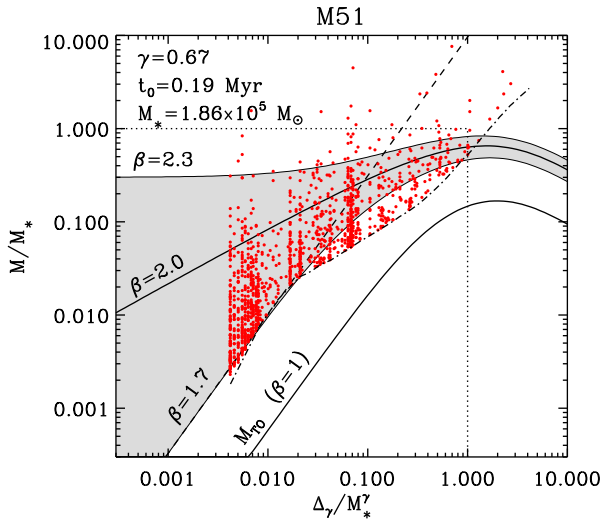


Figure 4. The time evolution of the mass where the evolved Schechter function has the logarithmic slope, $-\beta$, for $\beta = 1, 1.7, 2$ and 2.3 (same as in the right panel of Fig. 3). The dots are ages and masses of M51 clusters from B05, with the dot-dashed line defining the limiting mass due to a detection limit of 22.6 mag in the F435W filter. The dashed line shows $M(\beta = 1.7)$ when a continuous power law CIMF is assumed. The values of γ , t_0 and M_* , used to normalise the ages and masses to dimensionless units, follow from a maximum likelihood estimation (Section 4.1).

age of the M51 clusters in each age bin, being approximately 5 Myr, 50 Myr and 250 Myr for the panels (b), (c) and (d), respectively. The vertical offset is determined by A , and the best agreement is found for $A = 0.07 M_{\odot} \text{yr}^{-1}$. The coincidence of the empirical mass functions with the CIMF (dashed line) in the first two age bins, shows that the number of clusters per linear unit of time is approximately constant in the first 100 Myr. The implications of this will be discussed in more detail in Section 4.4. Only the dN/dM in the oldest age bin falls visibly below the CIMF. If a continuous power law distribution function would have been assumed for the CIMF, many more high-mass clusters would have to have been destroyed to make the model prediction agree with the data (already noted by Gieles et al. [2005] who do not include the most massive clusters when determining the disruption time of M51 clusters). The evolved Schechter functions describe the empirically derived mass functions very well and as could be seen already in Fig. 4, the turnover of the evolved Schechter functions remains well below the detection limit.

The empirical mass functions are also approximated by power laws and their indices, $-\beta_{\text{fit}}$, are indicated in each panel. The empirical mass functions in the first two age bins can be approximated by a power law with index of roughly -2 , but the oldest mass function is steeper. From a comparison to the (evolved) Schechter function, we see this is because the limiting mass approaches M_* at this age, where $\beta = 3$. On the low-mass end of the evolved Schechter function the effect of mass-dependent disruption is seen at old ages (panel [d]), where the mass function flattens to a logarithmic slope of $\gamma - 1 = -0.33$ and the turnover is at $M_{T0} \simeq 10^4 M_{\odot}$.

Though this is only an application to one data-set, it shows that a Schechter function evolved with mass-dependent disruption nicely describes empirically derived age and mass distributions.

The lack of a flattening of the empirical mass function at old ages, as compared to the CIMF_{emp} , is due the exponential truncation at high masses and the detection limit that shifts the mean observed masses closer to M_* , where the CIMF is steeper.

4.4 Age distributions for different mass cuts

Assuming a constant formation history of clusters, the cluster age distribution, $dN/d\tau$, can be found from a numerical integration of the evolved Schechter function from M_j to ∞ at each τ .

In panel (e) three (mass limited) age distributions are shown, for the three maximum ages, τ_j , and corresponding lower mass limit, M_j . The clusters are binned, such that the first bin starts at 4 Myr, the age of the youngest cluster, and the last bin ends at τ_j . The number of bins is chosen such that the bin widths are approximately constant for the three mass cuts. The number of clusters in each bin is counted and divided by the bin width, such that $dN/d\tau$ follows, i.e. the number of clusters per Myr.

Over-plotted as full lines are the age distribution resulting from the numerical integrations of the evolved Schechter functions again using the best-fitting parameters from the maximum likelihood estimate of Section 4.1. A single value of $A = 0.07 M_{\odot} \text{yr}^{-1}$, i.e. the same value as in Section 4.3, was used to describe all three age distributions. The different vertical offsets are caused by the different values of M_j . The good agreement between the model and the three empirical age distributions shows that both the disruption parameters and the CIMF shape, with the parameters from the model fit of Section 4.1, provide a good description of the cluster population of M51. With the value of A and the global SFR of M51 it is possible to derive Γ , i.e. the fraction of star formation occurring in star clusters that survive the embedded phase ($\text{CFR} = \Gamma \cdot \text{SFR}$, Bastian 2008). The global SFR of M51 is around $5 M_{\odot} \text{yr}^{-1}$ (e.g. Scoville et al. 2001). Since $\Gamma \cdot \text{SFR} = A E_1(M_{\text{min}}/M_*)$ (equation 6), with $E_1(M_{\text{min}}/M_*)$ roughly between 6 and 10, depending on M_{min} , the value of Γ resulting from this comparison is then $\Gamma \simeq 0.08 - 0.14$. So roughly 10% of the star formation in M51 occurs in star clusters that are detectable in the optical. This is in good agreement with the general finding of Bastian (2008) that $\Gamma = 0.08 \pm 0.03$ in different galactic environments.

The theoretical age distributions all show an initially flat part and then a rapid decline. For the lowest mass cut (M_1) the data do not allow us to verify this, due to the young age at which the $M_{\text{lim}}(\tau)$ line cuts the sample ($\tau_1 = 10$ Myr). The $dN/d\tau$ of the sample with the highest mass cut nicely shows this flat part and the decline. The solutions for the mass limited age distributions can be approximated within $\sim 10\%$ accuracy by

$$\frac{dN}{d\tau}(M > M_j) \simeq \frac{A}{M_*} \left(\frac{t_*^{\text{tot}}}{\tau + t_j^{\text{tot}}} \right)^{1/\gamma} E_2 \left(\frac{M_j}{M_*} \right) \exp(-2\tau/t_*^{\text{tot}}) \quad (30)$$

where t_*^{tot} is the total disruption time of a cluster with an initial mass M_* and t_j^{tot} is the same for a cluster with an initial mass M_j . This approximation only holds for an initial power law index of -2 at low masses. The approximation in equation (30) has the $\tau^{-1/\gamma}$ scaling predicted by BL03 for a continuous power law mass function, but it falls off faster (exponentially) at old ages, due to the truncation in the CIMF.

A flat part in $dN/d\tau$ at young ages is a typical result of the MDD model (BL03), although BL03 present the age distributions for luminosity limited cluster samples, which decline at young ages

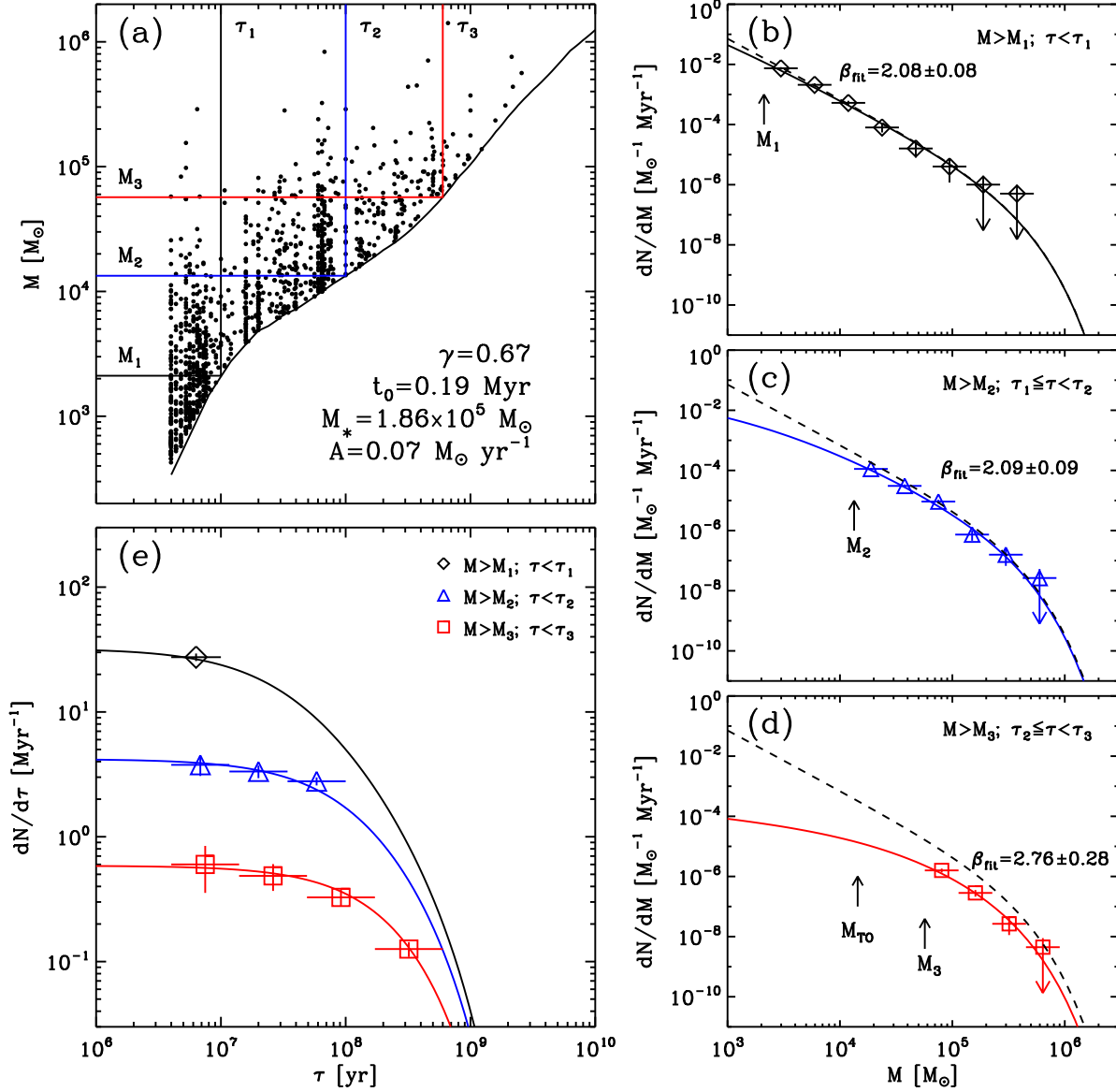


Figure 5. Ages and masses of M51 clusters (panel [a]) and the resulting mass functions in different age bins (panels [b]–[d]) with the evolved Schechter functions (equation 26) over-plotted. The parameters were determined by a maximum likelihood fit of the model to the data (Section 4.1). The empirical mass functions are approximated by power laws and the resulting index, $-\beta_{\text{fit}}$, is indicated in each panel. The mass limited age distributions for different mass cuts are shown in panel (e). The vertical positioning of the age distributions with respect to one another is due to the fact that each sample has a different lower mass limit (M_j). All mass functions and age distributions are described by a single value of $A = 0.07 M_{\odot} \text{yr}^{-1}$, corresponding to $\Gamma \simeq 0.1$, i.e. 10% of the star formation in M51 occurs in star clusters.

as $\tau^{-\zeta}$ due to evolutionary fading of clusters. In the prediction for $dN/d\tau$ in this study the evolutionary fading does not enter because for each age distribution a lower mass limit is adopted that is above the fading line (Fig. 5). A flat $dN/d\tau$ was also found for a mass limited sub-sample of clusters in the SMC up to almost a Gyr (Gieles et al. 2007). Indirect evidence for a flat $dN/d\tau$ for clusters in different galaxies follows from the linear scaling of $M_{\text{max}}(\log \tau)$

with τ in the first 100 Myr (Section 2.1.1 and Gieles & Bastian 2008).

Note that there is no evidence for ‘infant mortality’ from the $dN/d\tau$ in the first ~ 10 Myr, as was reported by B05 from the same data set. B05 used slightly smaller age bins and found evidence for a drop of a factor of four between the first age bin ($\lesssim 10$ Myr) and the second age bin. They also report an enhancement of clus-

ters around 60 Myr, which coincides with the moment of the last encounter between M51 and the companion galaxy (NGC 5195). However, there is an artificial age gap between 10 Myr and 20 Myr in the $dN/d\tau$, which is a common feature when broad-band photometry is used to derive ages (Gieles et al. 2005; Lee et al. 2005; Whitmore et al. 2007). These three effects average out when using slightly larger age bins and the details in the $dN/d\tau$ reported by B05 are not separable anymore. The difference between the first and the second bin for the sample with the highest mass cut is within 1σ still consistent with a decrease of a factor of two or three. However, panel (e) of Fig. 5 shows that a flat $dN/d\tau$ up to ~ 100 Myr describes the data very well.

Since this is a quite different interpretation of the data than what was concluded by B05, caused by a difference in how the data are binned, it is interesting to have a closer look at the $dN/d\tau$ of massive clusters with a method that does not rely on binning. One way of doing that is by creating a cumulative distribution function (CDF), which can then be compared to different models using a Kolmogorov-Smirnoff (K-S) test. In Fig. 6 the CDF of the first 100 Myr of the $dN/d\tau$ of clusters more massive than $M_3 \simeq 6 \times 10^4 M_\odot$ (Fig. 5) is shown (dots). The best-fitting model from Section 4.1 is shown as a full line. The null hypothesis that the data have been drawn from this model cannot be rejected. The K-S probability is 10%, i.e. the model is within 2σ consistent with these data.

Whitmore et al. (2007) claim that cluster evolution is ‘universal’ in the first 100 Myr and that the fraction of disrupted clusters in this period is independent of environment and mass. In their model, 90% of the clusters gets destroyed each age dex, resulting in a τ^{-1} scaling of the $dN/d\tau$ for mass limited samples. The CDF of this model is shown as a dashed line in Fig. 6. The K-S probability for the Whitmore et al. model is 2×10^{-8} and the hypothesis that these data are drawn from a τ^{-1} age distribution can, therefore, be safely reject. Even if the disruption fraction is lowered to 80% (70%), resulting in $dN/d\tau \propto \tau^{-0.7}(\tau^{-0.5})$ (Whitmore et al. 2007), the K-S probability is $6 \times 10^{-5}(10^{-3})$.

The fact that the full optically selected cluster population of M51 can be described by a CFR that is roughly 10% of the SFR indicates that *if* all stars form in embedded clusters, 90% of them are destroyed when the residual gas of the star formation process is removed and that this process lasts only a few Myrs. And it seems that ‘infant mortality’ does not affect the optically detected clusters and that information on the number of embedded clusters is needed to estimate the ‘infant mortality rate’, as was also done for the clusters in the solar neighbourhood (Lada & Lada 2003).

5 CONCLUSIONS AND DISCUSSION

This study considers the early evolution (first \sim Gyr) of the star cluster mass function, with particular focus on the mass range that is available through observations. A Schechter type function, i.e. a power law with an exponential truncation (equation 1), is used for the cluster initial mass function (CIMF). The use of this function is motivated by observational indications that the high-mass end of the CIMF of young extra-galactic clusters is steeper than the ‘canonical’ -2 power law (Gieles et al. 2006a; Larsen 2008). The exponential truncation provides a good description

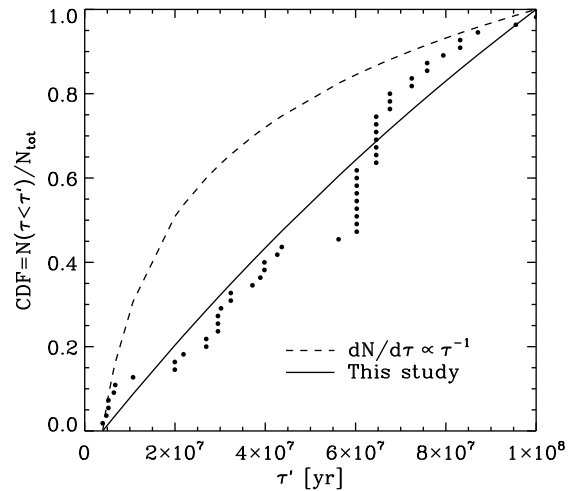


Figure 6. Cumulative distribution function (CDF) of ages (≤ 100 Myr) for the most massive clusters ($M \geq M_3 \simeq 6 \times 10^4 M_\odot$). The dashed and full lines show the CDF for the 90% MID model of Whitmore et al. (2007) and the one presented in this study, respectively.

of the high-mass tail of the globular cluster mass function (e.g. McLaughlin & Pudritz 1996).

Empirical cluster masses are generally found to be higher at older (logarithmic) ages. This is an observational bias because of two effects: the rapid fading of star clusters with age, making it increasingly more difficult to see low-mass clusters with increasing age; also, masses increase due to a size-of-sample effect, since longer time intervals are considered at higher logarithmic ages. If the CIMF has indeed an exponential truncation, this means that at older (logarithmic) ages the steepening is more noticeable than at young ages.

The shape of the cluster mass function at different ages depends on the functional form of the CIMF and the way clusters lose mass due to disruptive effects. Two competing models exist for the evolution of clusters, a mass-dependent disruption model (MDD, e.g. Boutloukos & Lamers 2003) and a mass-independent disruption model (MID, e.g. Whitmore et al. 2007) and both assume that star cluster masses are drawn from a continuous power law distribution with index -2 .

In this contribution a Schechter function is used for the CIMF, with a power law index of -2 at low masses and an exponential truncation at M_* (equation 1), which is evolved with mass-dependent cluster disruption. In summary, it is found that

- the exponential truncation of the Schechter function is not necessarily detectable from a small cluster sample, the kind that is used to create the mass function of clusters younger than ~ 10 Myr (here referred to as CIMF_{emp}), because in this short time interval there are generally not enough clusters sampled above M_* ;
- the age distribution of mass limited sub-samples is flat during the first ~ 100 Myr (depending on the mass cut and the disruption time-scale) and drops exponentially at older ages. Through a comparison to ages and masses of clusters in M51, it is shown that this holds for a sub-sample of clusters more massive than $6 \times 10^4 M_\odot$. The τ^{-1} age distribution, proposed by Whitmore et al. (2007) as

the result of a ‘universal’ cluster disruption model, is ruled out at high significance for these data;

- the mass for which the logarithmic slope of the evolved Schechter function is -2 increases with age as $\tau^{0.6}$. This scaling is similar to the increase of the limiting cluster mass, $M_{\text{lim}}(\tau)$, due to the evolutionary fading of clusters. This means that the mass function of clusters above the detection limit is approximately a power law with index -2 at all ages.

The MDD model, based on a continuous (nontruncated) power law CIMF, predicts that the mass function at old ages should have a logarithmic slope of $\gamma - 1 \simeq -0.35$ (Lamers et al. 2005a), while empirically derived mass functions at old ages are power laws with indices of approximately -2 , or even steeper (e.g. de Grijs & Anders 2006). This weakness of the MDD model was at the same time a supporting argument for the MID model. However, in this study it is shown that a power law mass function with index -2 at old ages results naturally when a Schechter type CIMF is assumed. This is illustrated in Section 4, where it is shown that a Schechter function evolved with mass-dependent disruption provides an excellent description of the (mass limited) age distribution and the mass function at different ages for star clusters in M51. The power law mass function of M51 clusters gets steeper with age, from an index of -2 at the youngest ages to an index of -2.8 at ~ 250 Myr. However, simultaneous fitting of models with different CIMF and disruption parameters to the ages and masses shows that the disruption time depends on mass as $t_{\text{dis}} \propto M^{0.67 \pm 0.06}$. This means that the logarithmic slope of the CIMF that is observable at ~ 250 Myr is smaller than -2.8 (i.e. steeper), since it has already been affected by disruption.

It would be interesting to apply the evolved Schechter function to more cluster populations for which age and mass information is available. As demonstrated in Section 4.1, the fundamental parameters defining a cluster population, namely M_* of the CIMF and t_0 and γ of the disruption law (equation 22) can easily be determined from luminosity limited cluster samples using a maximum likelihood estimate. Parmentier & de Grijs (2008) apply the MDD model to the age and mass distributions of LMC clusters and conclude that it is hard to constrain the disruption time-scale. They find that models with a long disruption times ($\gtrsim 1$ Gyr) are needed to describe the mass function, while short disruption times ($\lesssim 1$ Gyr) are preferred for the age distribution. Larsen (2008) showed that an exponential truncation in the CIMF around $2 \times 10^5 M_{\odot}$ provides a good description of the mass function of LMC clusters. Perhaps the disruption time-scale of LMC clusters can be better constrained when the evolved Schechter function from Section 3.2 is used.

Most probably the model presented in this paper will not be able to explain the age distribution of clusters in the Antennae galaxies (Fall et al. 2005). The τ^{-1} scaling of the age distribution and the mass-independent nature of the disruption model invoked to explain this is very peculiar and this has not been found in other galaxies thus far. Since the galactic environment in the Antennae galaxies is quite different than that of a quiescent spiral galaxy, it could be that clusters suffer from different (additional) mechanisms that disrupt clusters of different masses equally fast. Something along these lines was recently suggested by Renaud et al. (2008) who studied Antennae like mergers with N -body simulations. They show that due to the interaction of the two spiral discs there are strong compressive tides that probably induce star and cluster formation. Their models show that *if* clusters or associa-

tions indeed form in such compressive tides, they can be held together for 10 Myr or longer, thereby postponing the dissolution of clusters due to gas removal, which in other galaxies seems to destroy the majority ($\sim 90\%$) of the embedded clusters within a few Myrs after formation. Although this is speculative, it is important to keep in mind that the cluster system of the Antennae galaxies has very different properties as compared to other cluster systems (see the discussion in Gieles & Bastian 2008). Larsen (2008) showed that the CIMF of (normal quiescent) spiral galaxies can be well described by a Schechter function with $M_* \simeq 2 \times 10^5 M_{\odot}$. It should be possible to describe most of the age and mass distributions in (quiescent) galaxies with the model presented in this study.

To validate the correctness of the model presented in this study, it would be convincing to ‘detect’ the turnover in the mass function at ages between ~ 500 Myr and ~ 1 Gyr. From Fig. 4 it can be seen that the depth of observations available at the moment, would have to be increased by roughly one dex in mass, or 2.5 magnitude, to bring the turnover mass, M_{TO} , above the detection limit. The improved sensitivity of the new HST/WFC3 camera will allow us to trace the cluster mass function at old ages to the required depth to derive a mass function at intermediate ages down to the turnover ($M_{\text{TO}} \simeq 10^4 M_{\odot}$) for cluster populations at distances of $5 - 10$ Mpc.

ACKNOWLEDGEMENT

MG enjoyed stimulating discussions with Andrés Jordán and thanks Nate Bastian, Iraklis Konstantopoulos, Henny Lamers and Søren Larsen for discussions and critical reading of earlier versions of this manuscript.

REFERENCES

- Anders P., Fritze-v. Alvensleben U., 2003, *A&A*, 401, 1063
 Bastian N., 2008, *MNRAS*, 390, 759
 Bastian N., Gieles M., Lamers H. J. G. L. M., Scheepmaker R. A., de Grijs R., 2005, *A&A*, 431, 905 (B05)
 Bastian N., Saglia R. P., Goudfrooij P., Kissler-Patig M., Maraston C., Schweizer F., Zoccali M., 2006, *A&A*, 448, 881
 Baumgardt H., 2001, *MNRAS*, 325, 1323
 Baumgardt H., Kroupa P., Parmentier G., 2008, *MNRAS*, 384, 1231
 Baumgardt H., Makino J., 2003, *MNRAS*, 340, 227
 Benedict G. F., Howell D. A., Jørgensen I., Kenney J. D. P., Smith B. J., 2002, *AJ*, 123, 1411
 Bik A., Lamers H. J. G. L. M., Bastian N., Panagia N., Romaniello M., 2003, *A&A*, 397, 473
 Billett O. H., Hunter D. A., Elmegreen B. G., 2002, *AJ*, 123, 1454
 Boutloukos S. G., Lamers H. J. G. L. M., 2003, *MNRAS*, 338, 717 (BL03)
 Burkert A., Smith G. H., 2000, *ApJ*, 542, L95
 Cerviño M., Luridiana V., 2004, *A&A*, 413, 145
 Chandar R., Fall S. M., Whitmore B. C., 2006, *ApJ*, 650, L111
 Clark J. S., Negueruela I., Crowther P. A., Goodwin S. P., 2005, *A&A*, 434, 949
 Davies B., Figer D. F., Kudritzki R.-P., MacKenty J., Najarro F., Herrero A., 2007, *ApJ*, 671, 781
 de Grijs R., Anders P., 2006, *MNRAS*, 366, 295

- de Grijs R., Anders P., Bastian N., Lynds R., Lamers H. J. G. L. M., O'Neil E. J., 2003a, *MNRAS*, 343, 1285
- de Grijs R., Bastian N., Lamers H. J. G. L. M., 2003b, *ApJ*, 583, L17
- de Grijs R., Goodwin S. P., 2008, *MNRAS*, 383, 1000
- Dolphin A. E., Kennicutt Jr. R. C., 2002, *AJ*, 123, 207
- Elmegreen B. G., Efremov Y. N., 1997, *ApJ*, 480, 235
- Elmegreen B. G., Falgarone E., 1996, *ApJ*, 471, 816
- Elmegreen D. M., Chromey F. R., McGrath E. J., Ostenson J. M., 2002, *AJ*, 123, 1381
- Fall S. M., Chandar R., Whitmore B. C., 2005, *ApJ*, 631, L133
- Fall S. M., Zhang Q., 2001, *ApJ*, 561, 751
- Feldmeier J. J., Ciardullo R., Jacoby G. H., 1997, *ApJ*, 479, 231
- Figer D. F., MacKenty J. W., Robberto M., Smith K., Najarro F., Kudritzki R. P., Herrero A., 2006, *ApJ*, 643, 1166
- Fukushige T., Heggie D. C., 2000, *MNRAS*, 318, 753
- Gieles M., Bastian N., 2008, *A&A*, 482, 165
- Gieles M., Bastian N., Lamers H. J. G. L. M., Mout J. N., 2005, *A&A*, 441, 949
- Gieles M., Baumgardt H., 2008, *MNRAS*, 389, L28
- Gieles M., Lamers H. J. G. L. M., Portegies Zwart S. F., 2007, *ApJ*, 668, 268
- Gieles M., Larsen S. S., Bastian N., Stein I. T., 2006a, *A&A*, 450, 129
- Gieles M., Larsen S. S., Scheepmaker R. A., Bastian N., Haas M. R., Lamers H. J. G. L. M., 2006b, *A&A*, 446, L9
- Gieles M., Portegies Zwart S. F., Baumgardt H., Athanassoula E., Lamers H. J. G. L. M., Sipior M., Leenaarts J., 2006c, *MNRAS*, 371, 793
- Gnedin O. Y., Ostriker J. P., 1997, *ApJ*, 474, 223
- Goudfrooij P., Gilmore D., Whitmore B. C., Schweizer F., 2004, *ApJ*, 613, L121
- Goudfrooij P., Schweizer F., Gilmore D., Whitmore B. C., 2007, *AJ*, 133, 2737
- Haas M. R., Gieles M., Scheepmaker R. A., Larsen S. S., Lamers H. J. G. L. M., 2008, *A&A*, 487, 937
- Harris W. E., Kavelaars J. J., Hanes D. A., Pritchett C. J., Baum W. A., 2008, *AJ*, accepted (arXiv:0811.1437)
- Hunter D. A., Elmegreen B. G., Dupuy T. J., Mortonson M., 2003, *AJ*, 126, 1836
- Hwang N., Lee M. G., 2008, *AJ*, 135, 1567
- Jordán A., McLaughlin D. E., Côté P., Ferrarese L., Peng E. W., Mei S., Villegas D., Merritt D., Tonry J. L., West M. J., 2007, *ApJS*, 171, 101 (J07)
- Kennicutt R. C., 1998, *ApJ*, 498, 541
- Konstantopoulos I. S., Bastian N., Smith L. J., Trancho G., Westmoquette M. S., Gallagher III J. S., 2008, *ApJ*, 674, 846
- Kruijssen J. M. D., Lamers H. J. G. L. M., 2008, *A&A*, 490, 151
- Kumai Y., Basu B., Fujimoto M., 1993, *ApJ*, 404, 144
- Lada C. J., Lada E. A., 2003, *ARA&A*, 41, 57
- Lamers H. J. G. L. M., Gieles M., 2006, *A&A*, 455, L17
- Lamers H. J. G. L. M., Gieles M., Bastian N., Baumgardt H., Kharchenko N. V., Portegies Zwart S., 2005a, *A&A*, 441, 117
- Lamers H. J. G. L. M., Gieles M., Portegies Zwart S. F., 2005b, *A&A*, 429, 173
- Larsen S. S., 2000, *MNRAS*, 319, 893
- Larsen S. S., 2002, *AJ*, 124, 1393
- Larsen S. S., 2004, *A&A*, 416, 537
- Larsen S. S., 2008, *A&A*, accepted (arXiv:0812.1400)
- Lee M. G., Chandar R., Whitmore B. C., 2005, *AJ*, 130, 2128
- Mandushev G., Staneva A., Spasova N., 1991, *A&A*, 252, 94
- Maraston C., Bastian N., Saglia R. P., Kissler-Patig M., Schweizer F., Goudfrooij P., 2004, *A&A*, 416, 467
- Maschberger T., Kroupa P., 2007, *MNRAS*, 379, 34
- Mayya Y. D., Romano R., Rodríguez-Merino L. H., Luna A., Carrasco L., Rosa-González D., 2008, *ApJ*, 679, 404
- McCrary N., Graham J. R., 2007, *ApJ*, 663, 844
- McLaughlin D. E., Pudritz R. E., 1996, *ApJ*, 457, 578
- Mengel S., Lehnert M. D., Thatte N., Genzel R., 2005, *A&A*, 443, 41
- Mengel S., Tacconi-Garman L. E., 2007, *A&A*, 466, 151
- Ostriker J. P., Gnedin O. Y., 1997, *ApJ*, 487, 667
- Ostriker J. P., Spitzer L. J., Chevalier R. A., 1972, *ApJ*, 176, L51+
- Parmentier G., de Grijs R., 2008, *MNRAS*, 383, 1103
- Piskunov A. E., Kharchenko N. V., Schilbach E., Röser S., Scholz R.-D., Zinnecker H., 2008, *A&A*, 487, 557
- Press W. H., Schechter P., 1974, *ApJ*, 187, 425
- Press W. H., Teukolsky S. A., Vetterling W. T., Flannery B. P., 1992, *Numerical recipes in FORTRAN. The art of scientific computing*. Cambridge: University Press, —c1992, 2nd ed.
- Renaud F., Boily C. M., Fleck J.-J., Naab T., Theis C., 2008, *MNRAS*, 391, L98
- Sarajedini A., Mancone C. L., 2007, *AJ*, 134, 447
- Schechter P., 1976, *ApJ*, 203, 297
- Schulz J., Fritze-v. Alvensleben U., Möller C. S., Fricke K. J., 2002, *A&A*, 392, 1
- Scoville N. Z., Polletta M., Ewald S., Stolovy S. R., Thompson R., Rieke M., 2001, *AJ*, 122, 3017
- Silk J., Takahashi T., 1979, *ApJ*, 229, 242
- Smith L. J., Bastian N., Konstantopoulos I. S., Gallagher III J. S., Gieles M., de Grijs R., Larsen S. S., O'Connell R. W., Westmoquette M. S., 2007, *ApJ*, 667, L145
- Spitzer L. J., 1958, *ApJ*, 127, 17
- Vesperini E., 2000, *MNRAS*, 318, 841
- Vesperini E., Heggie D. C., 1997, *MNRAS*, 289, 898
- Waters C. Z., Zepf S. E., Lauer T. R., Baltz E. A., Silk J., 2006, *ApJ*, 650, 885
- Weidner C., Kroupa P., Larsen S. S., 2004, *MNRAS*, 350, 1503
- Whitmore B. C., Chandar R., Fall S. M., 2007, *AJ*, 133, 1067
- Whitmore B. C., Schweizer F., Kundu A., Miller B. W., 2002, *AJ*, 124, 147
- Whitmore B. C., Zhang Q., Leitherer C., Fall S. M., Schweizer F., Miller B. W., 1999, *AJ*, 118, 1551
- Zepf S. E., Ashman K. M., English J., Freeman K. C., Sharples R. M., 1999, *AJ*, 118, 752
- Zhang Q., Fall S. M., 1999, *ApJ*, 527, L81